Microstructure Evolution of Ammonia-Catalyzed Phenolic Resin During Thermooxidative Aging

Dan-Dan Guo, Mao-Sheng Zhan, Kai Wang

Key Laboratory of Aerospace Materials and Performance, Ministry of Education, School of Materials Science and Engineering, Beihang University, No. 37 Xueyuan Road, Beijing 100191, China

Received 21 September 2011; accepted 27 November 2011
DOI 10.1002/app.36550
Published online in Wiley Online Library (wileyonlinelibrary.com).

ABSTRACT: The thermooxidative aging of ammonia-catalyzed phenolic resin for 30 days at 60–170°C was investigated in this article. The aging mechanism and thermal properties of the phenolic resin during thermooxidative aging were described by thermogravimetry (TG)–Fourier transform infrared (FTIR) spectroscopy, attenuated total reflectance (ATR)–FTIR spectroscopy, and dynamic mechanical thermal analysis. The results show that the C—N bond decomposed into ammonia and the dehydration condensation between the residual hydroxyl groups occurred during the thermooxidative aging. Because of the presence of oxygen, the methylene bridges were oxidized into carbonyl groups. After aging for 30 days, the mass loss ratio reached 4.50%. The results of weight change at high temperatures coincided with the results of TG–FTIR spectroscopy and ATR–FTIR spectroscopy. The glass-transition temperature (T_g) increased from 240 to 312°C after thermooxidative aging for 30 days, which revealed the postcuring of phenolic resins. In addition, an empirical equation between the weight change ratio and T_g was obtained. © 2012 Wiley Periodicals, Inc. J Appl Polym Sci 000: 000–000, 2012

Key words: ageing; degradation; FT-IR; resins

INTRODUCTION

Ammonia-catalyzed phenolic resin is the preferred matrix material for heat-resistant composite materials because of its ability to form char efficiently, which is at a rate of 50–70% during endothermic pyrolysis. Therefore, it plays an important role in the anti-ablative field.[1,2] The chemical reactions will occur in heat-resistant composite materials under high-temperature environments, including pyrolysis reactions (vacuum or inert gas environment) and thermooxidation reactions (aerobic environment), and this will lead to volume ablation.[3,4] These two reactions both occur in phenolic resins. In addition, the materials will suffer thermooxidative aging during long-term storage at room temperature. Therefore, the mechanism of thermooxidative aging for phenolic resin is important for the study of the ablation resistance and storage stability of carbon-fiber-reinforced phenolic resin composites.

Recent investigations of phenolic resins have mainly focused on the thermal degradation behavior in a nitrogen environment[5–9] and the thermooxidation behavior at high temperatures.[10,11] According to Morterra and Low,[12] even in the presence of an oxidizing atmosphere, oxidative degradation is not an important pyrolysis pathway.[13] In this study, the microstructural evolution of ammonia-catalyzed phenolic resin during thermooxidation aging at 60–170°C was studied by accelerated aging methods, which suggested that the oxidation of methylene bridges could occur at low temperatures, but the degradation of methylene bridges and carbonyl groups was an important pyrolysis pathway at high temperatures. In addition, an empirical equation of the relationship between the weight change ratio and the glass-transition temperature (T_g) was obtained, which could be used to evaluate the thermal properties of phenolic resins during thermooxidative aging.

EXPERIMENTAL

Preparation of the samples

The phenolic resin samples were manufactured by compression molding with the powder of phenolic resin at 180°C. Then, the samples were kept at 180°C for 5 h *in vacuo* for postcuring.

Characterization methods

Weight change

For quality testing, the dimensions of samples were 30 × 10 × 4 mm^3. The specimens were put into an air atmosphere at different temperatures and measured periodically. The aging behavior at five different temperatures, namely, 60, 85, 130, 150, and 170°C,

Correspondence to: M.-S. Zhan (zhanms@buaa.edu.cn).

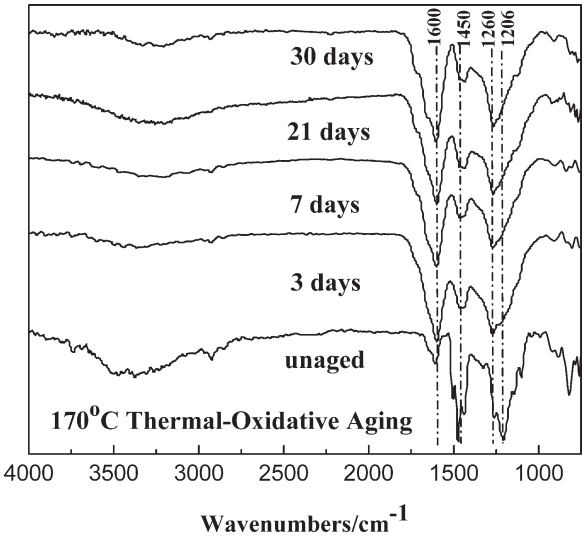

Figure 1 FTIR spectra of the phenolic resin samples after aging at 170°C in air.

was studied. The weight change ratio at any time (M_t) was calculated with the following equation:

$$M_t = (M_i - M_0)/M_0 \times 100\% \quad (1)$$

where M_i is the actual weight of the aging sample at time i and M_0 is the initial weight of the sample.

Characterization of the chemical structure

The samples after thermooxidative aging were analyzed by attenuated total reflectance–FTIR spectroscopy with a Nicolet spectrometer (model Nexus-470, Beijing, China).

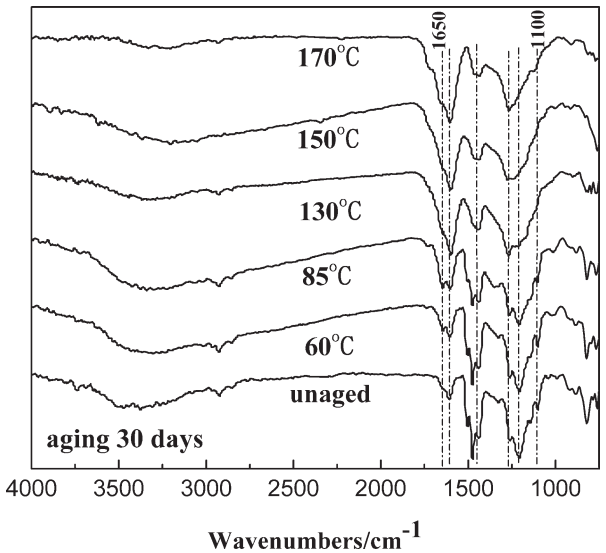

Figure 2 FTIR spectra of the phenolic resin samples after thermooxidative aging for 30 days: (a) TG and DTG curves for the phenolic resins and (b) DTG and Gram–Schmidt curves for the phenolic resins.

Thermooxidative degradation of the phenolic resins was analyzed with a thermogravimetric analysis (TGA)/FTIR system, which consisted of a TGA instrument (model Netzsch STA TGA-409C, Beijing, China) coupled to an FTIR system. Sample masses ranging from 15 to 20 mg were heated from 50 to 900°C at a rate of 10°C/min in a dry air atmosphere. IR spectra were recorded in the spectral range 4000–500 cm^{-1} with a resolution of 8 cm^{-1}.

Dynamic mechanical thermal analysis (DMTA)

DMTA was carried out with a dynamic mechanical thermal analyzer (model 2980, TA Instruments, Beijing, China), operating with a three-point bending clamp (flexural mode). The dimensions of the samples were 30 × 8 × 2 mm^3. The experimental conditions were a frequency of 1 Hz and a heating rate of 5°C/min.

RESULTS AND DISCUSSION

Infrared analysis

Figures 1 and 2 show the FTIR spectra of the phenolic resin samples after thermooxidative aging. The bands of ammonia-catalyzed phenolic resin are summarized in Table I.[14] The stretching band of phenolic OH shifted toward lower wave numbers for the original sample because of the H bonding formed between phenolic OHs.[15,16] Also, the band at 1100 cm^{-1} revealed the presence of C—N due to the reaction between ammonia and formaldehyde, which is described in the reaction shown in Scheme 1.[17]

The band at 1100 cm^{-1} decreased with the extension of aging time because of the cleavage of the C—N bond above 85°C. A new absorption appeared at 1650 cm^{-1} as a weak shoulder on the 1600-cm^{-1} doublet and was ascribed to the carbonyl groups produced through the oxidation of methylene bridges.[18] Also, the CH_2 band at 1450 cm^{-1} decreased in intensity for the same reasons. Indications of these changes could also be found in the

TABLE I
IR Bands and Assignments for the Ammonia-Catalyzed Phenolic Resin

Band position (cm^{-1})	Assignment
3300–3600	Phenolic OH stretching
2930	Aliphatic CH_2 asymmetric stretching
1673–1650	Carbonyl stretching
1610–1470	Quadrant ring stretching
1470–1440	Methylene CH_2 deformation
1240–1270	Phenol–phenol C—O stretching
1206–1240	Phenolic C—OH stretching
1100	C—N stretching
820	Out-of-plane ring deformation (1,2,4)
756	Out-of-plane ring deformation (1,2,6)

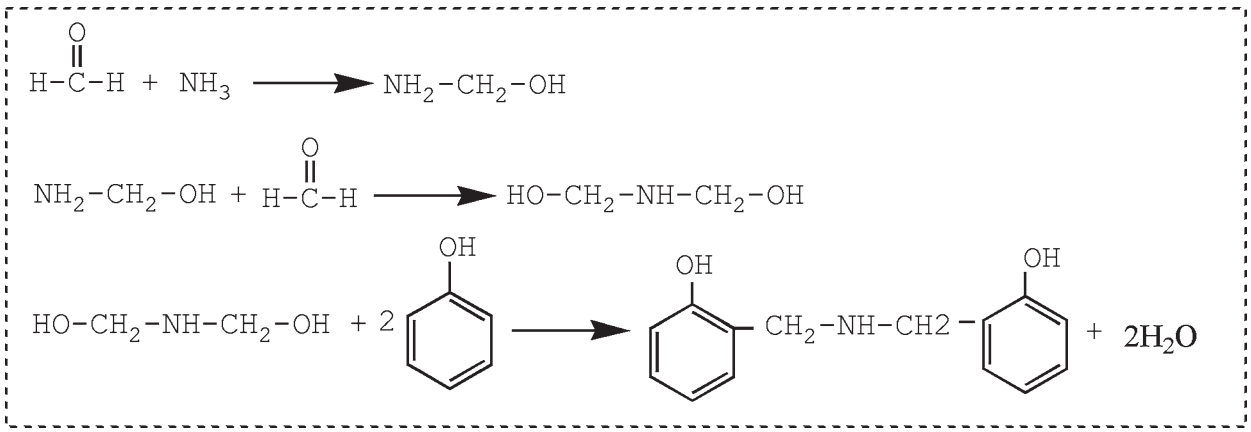

Scheme 1 Reaction between ammonia and formaldehyde.

growing band at 1600 cm^{-1} (aromatic ring stretching). The 3377-cm^{-1} peak (phenolic OH stretching) decreased, whereas the 1260-cm^{-1} peak (phenol–phenol C—O stretching) increased; this was attributed to phenolic OH—OH condensation.[19] In addition, there was no indication of the oxidation of phenolic OH from the FTIR spectra. Furthermore, the weak peaks at 756 and 820 cm^{-1} were determined to be caused by the condensation reaction between the residual hydroxymethyl groups and the aromatic ring.

Thermogravimetry (TG)/FTIR analysis

The TG weight loss curve and the corresponding derivative thermogravimetry (DTG) curve for the phenolic resins are shown in Figure 3(a). It was observed that the phenolic resins presented three weight loss regions at 251, 536, and 656°C. When the temperature reached 700°C, the rate of mass loss was almost constant. The final mass of the pyrolyzed sample was about 17% of its initial mass.

The Gram–Schmidt curve, which showed the intensity of all the gaseous decomposition products in the whole wave-number range, is compared with the DTG curve in Figure 3(b). Figure 4 presents the stacked FTIR spectra for the decomposition products of the phenolic resins at 251, 536, and 656°C in air. The peak positions of both curves coincide with each other in Figure 3(b). The first peak was attributed to the generation of NH_3. The second peak was caused by the postcuring and thermooxidative degradation of the phenolic resin with the evolution of H_2O, CO_2, and CO. The third one was due to the evolution of CH_4.[7] The last one was regarded as the char-formation reaction, which produced H_2O, CO, and CO_2.

The changes in the decomposition gases measured by FTIR and three-dimensional FTIR spectroscopy for the decomposition products of the phenolic resins with heat-treatment temperature are shown in Figures 5 and 6. It can be seen that NH_3, CH_4 and H_2O, CO, and CO_2 appeared during the thermooxidative degradation. The decomposition temperatures

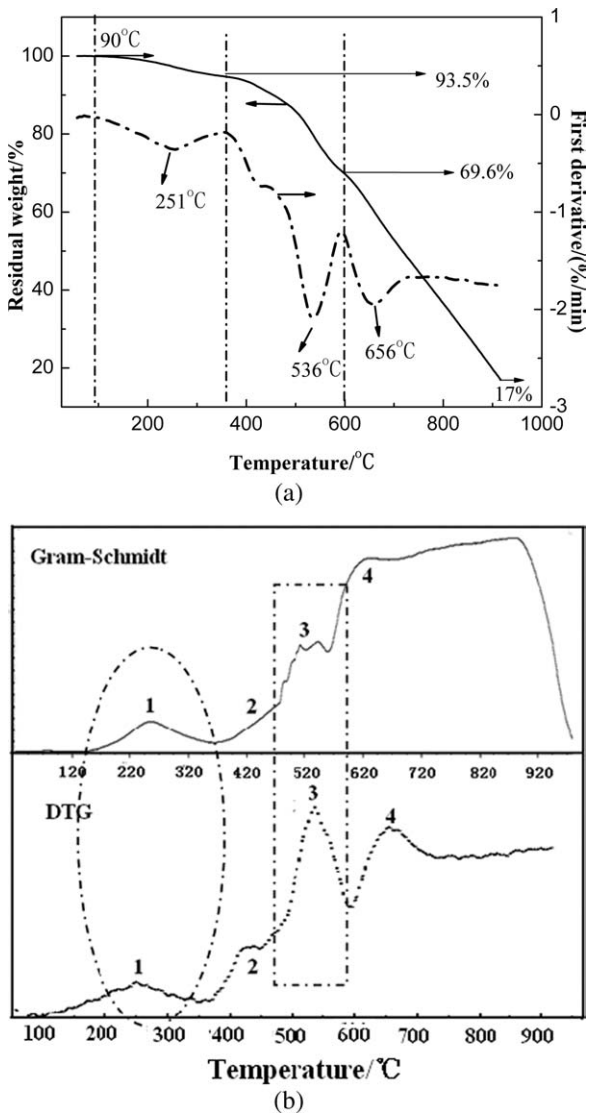

Figure 3 TG–DTG and Gram–Schmidt curves for the phenolic resins.

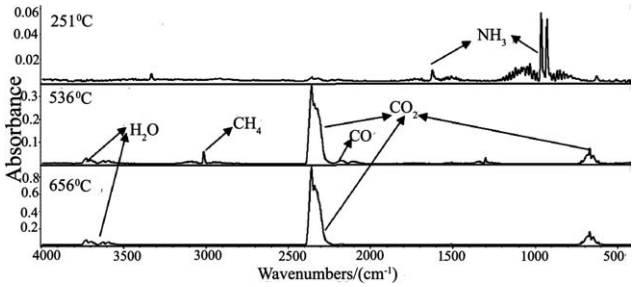

Figure 4 Stacked FTIR spectra for the decomposition products of the phenolic resins in air.

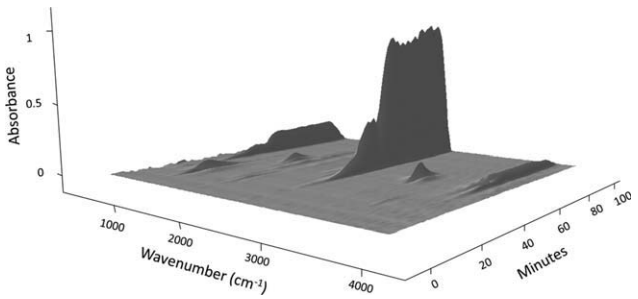

Figure 6 Three-dimensional FTIR spectra for the decomposition products of the phenolic resins.

of the phenolic resins are shown in Table II. It was noticed that the evolution of NH_3 suggested the changes in the absorption of the C—N bond shown in the FTIR spectra. The evolution of H_2O, CH_4, CO, and CO_2 were attributed to the postcuring, thermooxidative degradation, and char-formation reactions of the phenolic resins.

In conclusion, the chemical structure changes of ammonia-catalyzed phenolic resin during thermooxidative aging consisted of postcuring involving residual methylol groups that were still proceeding from the synthesis reaction, oxidation, and degradation. The degradation process could be viewed as a three-step decomposition. In the first decomposition stage (120–350°C), the C—N bond was removed with the evolution of NH_3, and additional crosslinks were formed as a result of condensation reactions involving a phenolic OH—OH condensation mechanism that yielded diphenyl ether linkages. In the second degradation stage (350–600°C), the methylene bridges and carbonyl groups were decomposed with the evolution of H_2O, CH_4, CO_2, and CO. In the third stage (>600°C), the char-formation reaction of the phenolic resins occurred and produced H_2O, CO, and CO_2. The amount of residue was 17% at 900°C. The thermooxidation reactions of ammonia-catalyzed phenolic resin are shown in Figure 7.

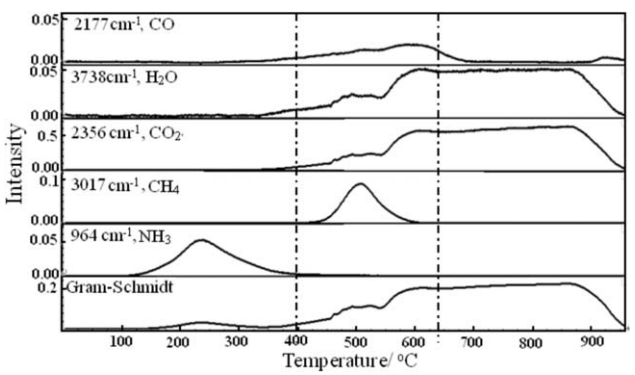

Figure 5 Changes in the decomposition gases measured by FTIR spectra with heat-treatment temperature.

Weight change

The M_t values obtained by gravimetry during the thermooxidative aging at different temperatures are shown in Figure 8. The results indicate that the higher the aging temperature was, the larger the weight change ratio was. The mass loss increased rapidly at the initial period of aging because of the loss of moisture and water produced during postcuring. Above 120°C, the mass decreased significantly; this was attributed to the generation of NH_3 and H_2O due to crosslinking. The results coincided with those shown in FTIR and TG/FTIR spectroscopy. The mass loss ratio reached 4.50% after 30 days of aging at 170°C.

The mathematical treatments of the experimental data of mass loss used the following empirical equation, which was revised according to Fick's law[20–22]:

$$M_t = a(T)\left(\sqrt{t}/h\right)^2 + b(T)\left(\sqrt{t}/h\right) + c(T) \qquad (2)$$

where t is the aging time, h is the thickness of the sample, and a, b, and c are parameters governed by the temperature.

In Table III, the values of parameters a, b, and c resulting from the mathematical treatments according

TABLE II
Main Gaseous Decomposition Products of the Phenolic Resin in Air

Gaseous decomposition product	T_i (°C)[a]	T_m (°C)[b]	T_f (°C)[c]
NH_3	125	250	400
H_2O	300	600	900
CH_4	450	525	600
CO	300	600	700
CO_2	300	600	900

[a] Initial releasing temperature of the gaseous decomposition product.
[b] Maximum releasing temperature of the gaseous decomposition product.
[c] Final releasing temperature of the gaseous decomposition product.

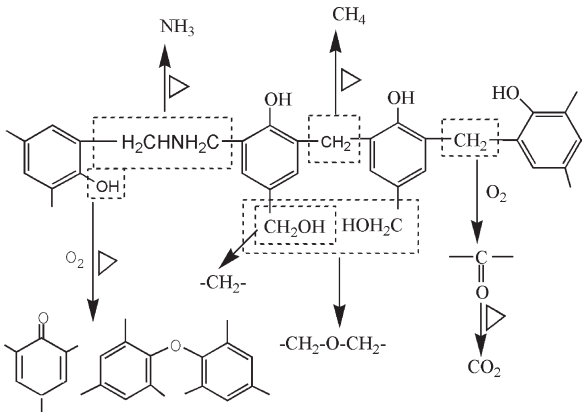

Figure 7 Thermooxidation mechanism of the ammonia-catalyzed phenolic resin.

to the empirical equation are shown. The relationships between the parameters (a, b, and c) and the aging temperature is shown in Figure 9 and can be expressed as the following functions:

$$a = e^{(-21.567-3179/T)} \quad (3)$$

$$b = e^{(-8.338-3041/T)} \quad (4)$$

$$c = 5.197 \times 10^4 + 3.143 \times 10^{-10} e^{3.57} 8 \times 1^{0-2T} \quad (5)$$

where T is the aging temperature. The mathematical relationship between the weight change ratio and the aging time can be expressed by the following revised equation:

$$M_t = e^{(-21.567-3179/T)}(\sqrt{t}/h)^2 - e^{(-8.338-3041/T)}(\sqrt{t}/h) + 3.14 \times 10^{-10} e^{3.578\times10^{-2}T} + 5.197 \times 10^{-4} \quad (6)$$

According to eq. (6), the mass loss of the phenolic resin during thermooxidative aging could be predicted.

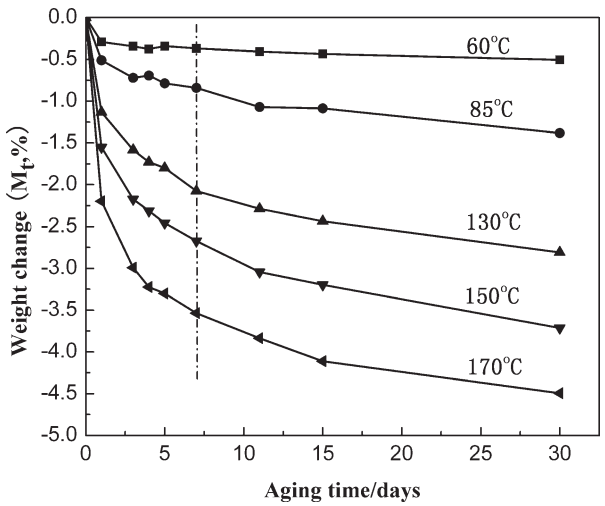

Figure 8 Weight change of the phenolic resin during thermooxidative aging.

TABLE III
Values of the Parameters Resulting from the Fitting

T	$1/T$ (K^{-1})	ln a (m^2/s)	ln $-b$ ($m/s^{1/2}$)	C (10^{-2})
60°C/333 K	0.003	−31.01	−17.541	0.0589
85°C/358 K	0.00279	−30.598	−16.757	0.0618
130°C/403 K	0.00248	−29.422	−15.834	0.106
150°C/423 K	0.00236	−29.127	−15.554	0.173
170°C/443 K	0.00226	−28.687	−15.241	0.292

DMTA

The curves of the loss angle tangent (tan δ) and the storage modulus (E') versus temperatures for the phenolic resin are present in Figure 10(a,b), respectively. It was noticed that E' decreased with the increase in heating treatment temperature first and then increased because of additional crosslinking. In addition, E' increased with the increase in aging temperature because of the postcuring of the phenolic resin during thermooxidative aging.[23]

As shown in Figure 10(a), T_g increased with the increase in aging temperature. T_g for the unaged

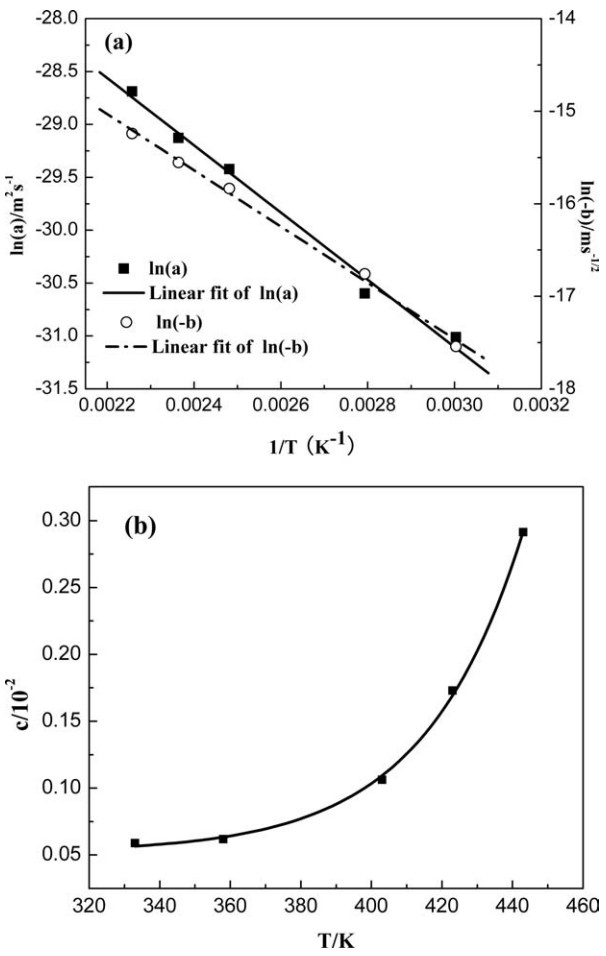

Figure 9 Fitting of the parameters in empirical eq. (2): (a) ln a versus the reciprocal absolute temperature and (b) c versus the absolute temperature.

sample was 240°C, and then, it rose to 312°C after 30 days of aging at 170°C. Figure 10(c) shows that T_g increased with the extension of aging time; this suggested the postcuring of the phenolic resin.

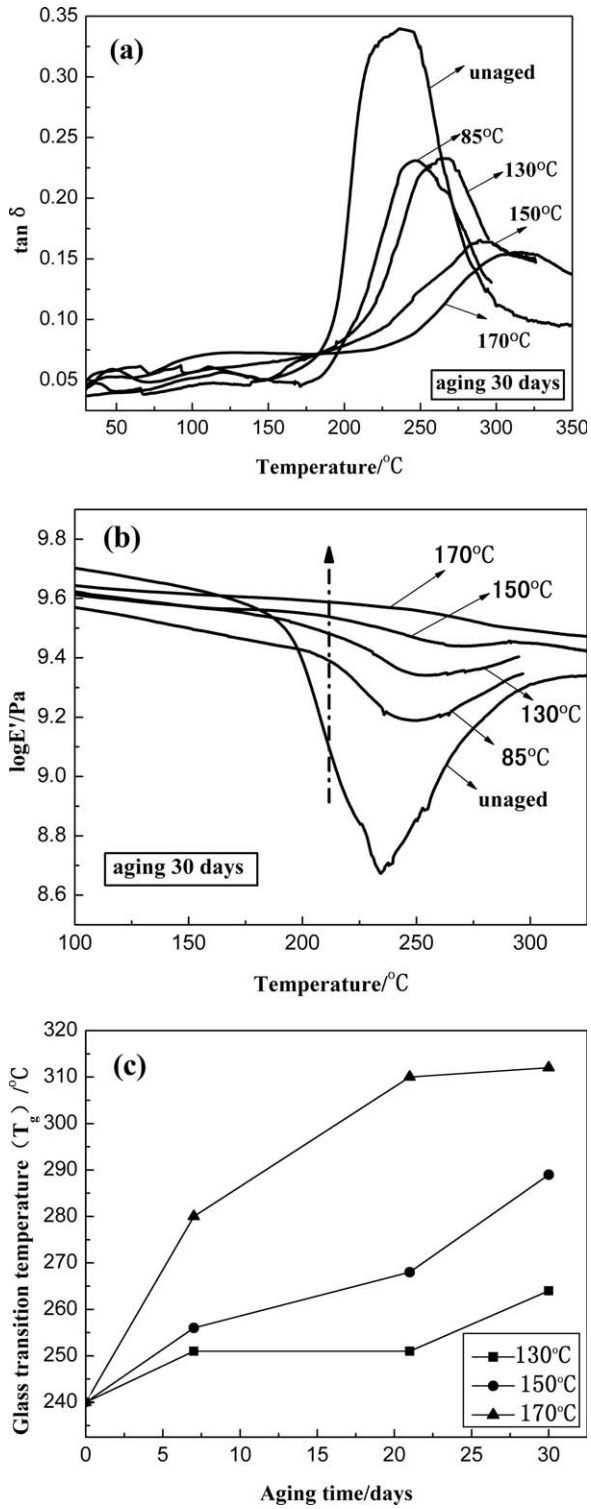

Figure 10 DMTA curves obtained for the phenolic resin: (a) tan δ versus the temperature, (b) E' versus the temperature, and (c) T_g versus the aging time.

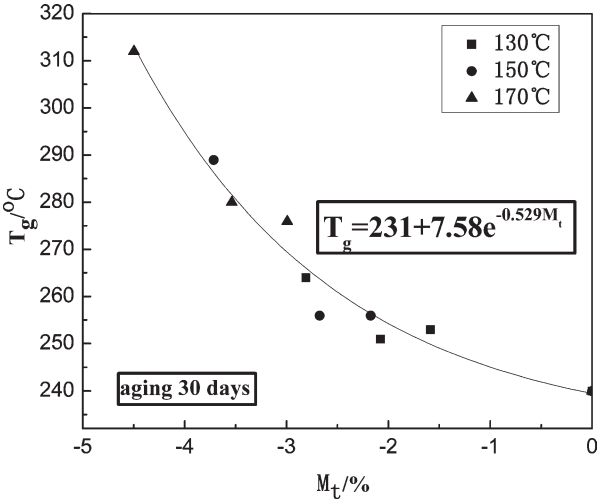

Figure 11 Relationship curve of T_g and M_t.

As we know, T_g is directly related to the crosslinking density of the thermosetting phenolic resin. The results of FTIR and TG/FTIR spectroscopy showed that the crosslinking density of the phenolic resin was affected by postcuring; this was attributed to the dehydration condensation between the residual hydroxyl groups and led to the weight loss of the phenolic resin. Therefore, the change in T_g was related to the mass loss, which was easily characterized.

Figure 11 shows the relationship between T_g and the mass loss of the phenolic resin. From Figure 11, we noticed that with the increase of mass loss, T_g increased; this was attributed to the moisture evaporation and postcuring of the phenolic resin. The relationship between T_g and the weight change ratio can be expressed by the following equation:

$$T_g = 231 + 7.58e^{-0.529Mt} (M_t \leq 0) \tag{7}$$

According to eqs. (6) and (7), a new function could be derived as follows:

$$\ln(T_g - 231) = 2.025 - 0.529\left(e^{-16.96-\frac{3179}{T}}(\sqrt{t/h})^2 - e^{-3.73-\frac{3041}{T}}(\sqrt{t/h}) + 3.14\times10^{-8}e^{3.578\times10^{-2}T} + 5.197\times10^{-2}\right) \tag{8}$$

This equation could be used to evaluate the change in T_g during thermooxidative aging.

CONCLUSIONS

1. The overall thermooxidative aging process of the ammonia-catalyzed phenolic resin consisted

of moisture evaporation and chemical structure changes. The oxidation of methylene bridges occurred at 60°C. The degradation process could be viewed as a three-step decomposition. In the first stage (120–350°C), the C—N bond was removed with the evolution of NH_3, and additional crosslinks were formed as a result of condensation reactions. In the second degradation stage (350–600°C), the methylene bridges and carbonyl groups were decomposed with the evolution of H_2O, CH_4, CO_2, and CO. In the third stage (>600°C), the char-formation reactions of the phenolic resins occurred and produced H_2O, CO, and CO_2. The amount of residue was 17% at 900°C.

2. The weight of the phenolic resin decreased after thermooxidative aging for 30 days at 60–170°C. Above 120°C, the mass decreased significantly; this was attributed to the postcuring of the phenolic resin. The mass loss ratio of the phenolic resin reached 4.50% after 30 days of aging at 170°C.
3. With the extension of aging time, the higher the aging temperature was, the higher T_g was. Finally, T_g increased from 240 to 312°C after 30 days of aging at 170°C. Moreover, an empirical relation between the weight change ratio and the aging time was obtained and could be used to evaluated the thermal properties of phenolic resins during thermooxidative aging.

References

1. Park, J. K.; Kang, T. J. Carbon 2002, 40, 2125.
2. Carotenuto, G.; Nicolais, L. J Appl Polym Sci 1999, 74, 2703.
3. Srikanth, I.; Daniel, A.; Kumar, S.; Padmavathi, N.; Singh, V.; Ghosal, P.; Kumar, A.; Devi, G. R. Scr Mater 2010, 63, 200.
4. Gabilondo, N.; Larrañaga, M.; Peña, C.; Corcuera, M. A.; Echeverría, J. M.; Mondragon, I. J Appl Polym Sci 2006, 102, 2623.
5. Zeng, H. Y.; Jiang, H.; Xia, K.; Wang, Y. J.; Huang, Y. Environ Sci Pollut Res 2010, 17, 1035.
6. He, G.; Riedl, B.; Aït-Kadi, A. J Appl Polym Sci 2003, 87, 433.
7. Kim, Y. J.; Kim, M. I.; Yun, C. H.; Chang, J. Y.; Park, C. R.; Inagaki, M. J Colloid Interface Sci 2004, 274, 555.
8. Trick, K. A.; Saliba, T. E. Carbon 1995, 33, 1509.
9. Chen, Y. F.; Chen, Z. Q.; Xiao, S. Y.; Liu, H. B. Thermochim Acta 2008, 476, 39.
10. Costa, L.; Montelera, L. R.; Camino, G.; Weil, E. D.; Pearce, E. M. Polym Degrad Stab 1997, 56, 23.
11. Jha, V.; Banthia, A. K.; Paul, A. J Therm Anal 1989, 35, 1229.
12. Morterra, C.; Low, M. J. D. Langmuir 1985, 1, 320.
13. Jackson, W. M.; Conley, R. T. J Appl Polym Sci 1964, 8, 2163.
14. Krıstkova, M.; Filip, P.; Weiss, Z.; Peter, R. Polym Degrad Stab 2004, 84, 49.
15. Wu, H.-D.; Ma, C.-C. M.; Chu, P. P. Polymer 1997, 38, 5419.
16. Li, J.; Li, S. J. Jpn Wood Res Soc 2006, 52, 331.
17. Gabilondo, N.; López, M.; Ramos, J. A.; Echeverría, J. M.; Mondragon, I. J Therm Anal Calorim 2007, 90, 229.
18. Nam, J.-D. Chairperson of the Supervisory Committee, 1991.
19. Costa, L.; Rossi di Montelera, L.; Camino, G.; Weil, E. D.; Pearce, E. M. Polym Degrad Stab 1997, 56, 23.
20. Cabanelas, J. C.; Prolongo, S. G.; Serrano, B. J. Mater Process Technol 2003, 143–144, 311.
21. Grave, C.; Mcewan, I.; Pethrick, R. A. Appl Polym Sci 1998, 69, 2369.
22. Mohd Ishak, Z. A.; Ariffin, A.; Senawi, R. Eur Polym J 2001, 37, 1635.
23. Munoz, J. C.; Ku, H.; Cardona, F.; Rogers, D. J Mater Process Technol 2008, 202, 486.